Effect of Poly(acrylic acid) Molecular Mass and End-Group Functionality on Calcium Oxalate Crystal Morphology and Growth

Christopher P. East,[1,2] Andrew D. Wallace,[1] Ali Al-Hamzah,[1] William O. S. Doherty,[2] Christopher M. Fellows[1]

[1]*School of Science and Technology, The University of New England, Armidale 2351, NSW, Australia*
[2]*Sugar Research and Innovation, Centre for Tropical Crops and Biocommodities, Queensland University of Technology, Brisbane, Queensland 4001, Australia*

Received 1 May 2009; accepted 11 August 2009
DOI 10.1002/app.31342
Published online 7 October 2009 in Wiley InterScience (www.interscience.wiley.com).

ABSTRACT: A number of series of poly(acrylic acids) (PAA) of differing end-groups and molecular mass were used to study the inhibition of calcium oxalate crystallization. The effects of the end-group on crystal speciation and morphology were significant and dramatic, with hexyl-isobutyrate end groups giving preferential formation of calcium oxalate dihydrate (COD) rather than the more stable calcium oxalate monohydrate (COM), while both more hydrophobic end-groups and less-hydrophobic end groups led predominantly to formation of the least thermodynamically stable form of calcium oxalate, calcium oxalate trihydrate. Conversely, molecular mass had little impact on calcium oxalate speciation or crystal morphology. It is probable that the observed effects are related to the rate of desorption of the PAA moiety from the crystal (lite) surfaces and that the results point to a major role for end-group as well as molecular mass in controlling desorption rate. © 2009 Wiley Periodicals, Inc. J Appl Polym Sci 115: 2127–2135, 2010

Key words: crystallization; polyelectrolytes; SEM (Scanning Electron Microscopy); XRD (X-Ray Diffraction)

INTRODUCTION

The control of calcium oxalate crystallization is a significant challenge in a number of different environments, including bleached wood pulp production[1] and *in vivo* within the urinary tract.[2–4] Our interest in calcium oxalate arises from the importance of calcium oxalate in cane sugar milling, where calcium oxalate monohydrate and dihydrate are major components of recalcitrant scaling in sugar mill evaporators.[5–10] The sources of calcium oxalate in sugar mills are calcium hydroxide (added to the juice in the clarification stage), and oxalic acid, which is both originally present in the sugar cane and formed *in situ* by oxidation of sucrose.[11]

Three hydrate forms of calcium oxalate are commonly encountered when the salt is precipitated from aqueous solution: calcium oxalate monohydrate (Whewellite, COM), dihydrate (Weddellite, COD), and trihydrate (Caoxite, COT). In pure aqueous solution, calcium and oxalate ions typically precipitate to give COM as the final product, via a COT intermediate. The speciation observed is highly dependent on experimental conditions—it is possible to obtained predominantly any one of the three hydrates from a feed of identical overall composition with changes in mixing procedure alone.[12] In general high initial $[Ca^{2+}]/[C_2O_4^{2-}]$ ratios, lower temperatures, and the presence of carboxylic acid[13] favor the formation of COD and COM over COT.[14]

At 23°C, the temperature used in this work, estimated K_{sp} values are 1.7×10^{-9} for COM, 4.2×10^{-9} for COD, and 5.4×10^{-9} for COT, based on trendlines for a large set of published data between 10°C and 50°C.[15] These solubility products are for a system containing only water, calcium ions, and oxalate ions. At high supersaturations, a greater fraction of COD is reported to form,[14] and the effect of increasing univalent cation concentration is generally to increase the solubility product.[15]

A great deal of work has been done using polyelectrolyte additives to inhibit and control the precipitation of these salts, chiefly under the low temperature conditions appropriate for the prevention of calculi in the urinary tract.[16–19] Although these studies have investigated numerous polymers and copolymers of both biological and synthetic origin, the sugar industry is restricted by regulatory constraints to a small palette of poly(carboxylic acid) additives, chiefly poly(acrylic acid) (PAA) and poly (maleic acid). The molecular mass has been the

Correspondence to: C. M. Fellows (cfellows@une.edu.au).

Figure 1 Polymeric scale inhibitors prepared. EB, $n = 1$; HB, $n = 5$; DB, $n = 7$; HDB, $n = 15$.

only easily altered parameter for these species, and there is abundant evidence that the most effective calcium oxalate scale inhibition is found in the molecular mass range 2000–4000, the same molecular mass range where maximum absorption of polyacrylate salts to calcium carbonate has been observed.[20,21]

In previous work, we have reported on the effect of sucrose, silica, and calcium and magnesium ion concentrations on calcium oxalate formation,[5,11] and have investigated the effect of polymeric additives on the inhibition of calcium oxalate crystallization under conditions designed to simulate cane sugar mill process streams.[22] The results of Yu et al. (2005) showed that the presence of silica, and to a certain extent, sucrose, selectively stabilized COD or COT as opposed to COM. The proportions of COD and COT, and the crystal size and habit of COM were dependent on the concentrations of silica and sucrose. Yu et al. (2005) attributed the differences observed to differences in adsorption capabilities of the various crystal phases of calcium oxalate for silica and sucrose macromolecules. Doherty (2006) found that magnesium ions significantly enhance the solubility of calcium oxalate. The addition of sucrose at up to 7% w/w was found to slightly increase the apparent solubility product of calcium oxalate, but higher concentrations led to a significant decrease in solubility product and the formation of less regular COM crystals with a serrated morphology.[11]

Doherty et al. (2004) reported on the effect of the end-group functionality and molecular mass of PAA in inhibition of crystallization of calcium oxalate in synthetic sugar juices.[22] These PAA were prepared using radical polymerization with conventional thiol chain transfer agents in order to control molecular mass and end-group functionality, and the effectiveness of the additives in reducing crystallization was found to improve with the hydrophilicity of the end-groups. The goal of the present work is to validate and extend these observations by preparing polymers of narrow polydispersity and controlled end-group composition using controlled radical polymerization. The narrow polydispersities obtainable by controlled radical polymerization methods such as Atom Transfer Radical Polymerisation (ATRP) will clarify the effects of molecular mass on inhibition efficiency, while the ease with which ATRP initiators may be modified provides a facile means of incorporating a variety of end-group functionalities. PAA scale inhibitors were therefore prepared in the molecular mass range 1200–16,000, with a variety of end-groups derived from the ATRP initiator, and tested for their ability to inhibit calcium oxalate precipitation and affect calcium oxalate crystal morphology.

EXPERIMENTAL

The synthesis and characterization of the PAA scale inhibitors used via ATRP of *tert*-butyl acrylate (BA) has been described in an accompanying publication.[23] PAA terminated with ethyl isobutyrate (EB), *n*-hexyl isobutyrate (HB), cyclohexyl isobutyrate (CB), *n*-decyl isobutyrate (DB), and *n*-hexadecyl isobutyrate (HDB) were prepared (Fig. 1). The molecular mass of these polymers was determined using ^{1}H-NMR (through quantification of the ^{1}H signal from end-groups and polymer backbone to give a number average molecular mass, M_N) and by size exclusion chromatography (SEC) of poly(BA) precursors. The estimated molecular mass averages and polydispersities for all PAA studied are summarized in Table I.

The number average molecular masses determined by ^{1}H-NMR and SEC were in broad agreement with the values predicted from the monomer:initiator ratios used in the ATRP synthesis.

EXPERIMENTAL MEASUREMENTS

Filtered distilled water (204 mL, 0.45 μm cellulose acetate membrane) was placed in a 400 mL reaction vessel and stirred magnetically. Ten mL of a 1000 ppm solution of Ca^{2+} (as $CaCl_2$) was added and the solution was allowed to equilibrate for 1 min, after which 10 mL of a 1570 ppm solution of $C_2O_4^{2-}$ (as

TABLE I
Molecular Masses of PAA Determined by ^{1}H-NMR and SEC

PAA	M_N (^{1}H-NMR)	M_N (SEC)	M_W (SEC)	PDI
EB 1	1669	1598	2091	1.3
EB 2	5065	4548	6029	1.3
EB 3	7180	5242	6625	1.3
HB 1	1981	1864	2177	1.2
HB 2	4224	2879	3396	1.2
HB 3	6723	3307	3856	1.2
CB 1	1852	1714	2136	1.3
CB 2	3518	2367	2867	1.2
CB 3	6210	3399	4092	1.2
DB 1	2422	2392	3072	1.3
DB 2	4472	3064	3816	1.3
DB 3	6203	2717	4074	1.5
HDB 1	1687	n/d	n/d	n/d
HDB 2	4135	n/d	n/d	n/d
HDB 3	9391	n/d	n/d	n/d

PDI = Polydispersity Index.

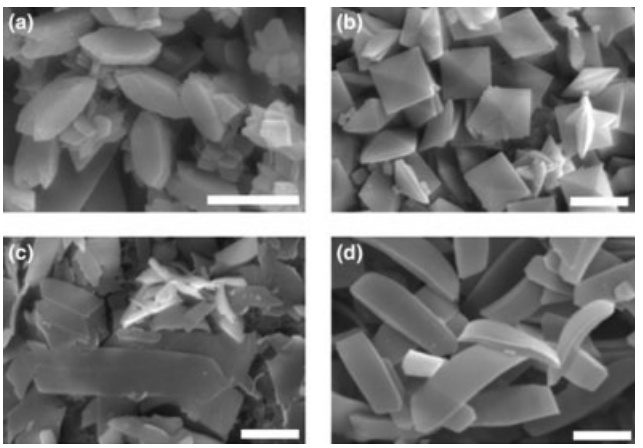

Figure 2 Representative calcium oxalate crystal morphologies. (a) COM from Control, 80 min. (b) COD from Series 1, HB1, 120 min. (c) COT from Control, 30 s. (d) Plate-like COT from Series 2, CB2, 80 min. Length of the scale bars is 5 μm in all micrographs.

$Na_2C_2O_4$) was added. Twenty-five mL of 5.4 ppm polymer solution was added to the reaction vessel either at the same time as the $CaCl_2$ solution (Series 1) or 30 s after the addition of $Na_2C_2O_4$ solution (Series 2). This procedure gave final molar concentrations of 1.0 m*M* Ca^{2+} and 0.71 m*M* $C_2O_4^{2-}$ and 0.54 ppm PAA. The concentrations of polymer, calcium, and oxalate ions used for this study were in the same proportion as typically encountered in a sugar factory where defecation is the method of juice clarification.[22] A limited series of experiments following the Series 1 procedure were also carried out at 90°C.

Series 1 was intended to observe the effect of the additives on both growth and nucleation of crystals, while Series 2 was intended to isolate the effect of the additives on the growth of crystal nuclei already present. The tests were allowed to run for 2 h at 22 ± 1°C and 6 mL aliquots were taken at 2, 40, 80 and 120 min. These aliquots were filtered though a 0.45 μm cellulose acetate membrane and the crystals analysed by Scanning Electron Microscopy (SEM) and X-ray powder diffraction (XRD). The proportions of the calcium oxalate phases in the precipitate were estimated from the intensity ratios of the major XRD lines.[12] SEM images were obtained from gold-coated samples using a JSM-5800 SEM situated at the Electron Microscope Unit, University of New England and XRD was carried out using a PANalytical, 'X' Pert PRO at the X-Ray Analysis Facility, Queensland University of Technology.

RESULTS

Typical crystal polymorph morphologies

X-ray powder diffraction of the precipitated calcium oxalates in the presence and absence of PAA were carried out to identify the three main calcium oxalate phases.[12]

Figure 2 shows representative SEM micrographs of the main calcium oxalate crystal morphologies obtained in this study. The observed morphologies are consistent with the reported boat/coffin morphology of COM,[24,25] the bipyramidal morphology of COD,[26] and plate-like morphology of COT.[12]

Another COD morphology, observed in the presence of most of the polymer additives, was small elongated COD crystals. This morphology has been reported previously, with the COD polymorph confirmed by Zhang et al.[26] The morphology changes as shown in Figure 3 (crystal sizes not to scale).

Crystal morphologies in the absence of PAA

In control experiments, the formation of all three polymorphs could be observed after 30 s of crystallization with COT clearly dominant. Both COD and boat COM were evident, but with crystals small and poorly formed. After 2 min, COT crystals had typically grown into large plates and the boat COM and COD crystals also grew considerably and became more clearly formed. In samples taken at 40 min, the COT had largely disappeared, apparently redissolved and recrystallized to give a large amount of COM with a clear boat morphology. A small amount of COD was also present. At long times, the control experiments showed well-formed crystals of COM and COD and stellates arising from heterogeneous nucleation (Fig. 4) and was confirmed to be primarily COM by XRD.

These results are consistent with Ostwald's Rule of Stages,[27] which suggests that in most cases the first crystal polymorph to form will be the one which requires the least structural change on

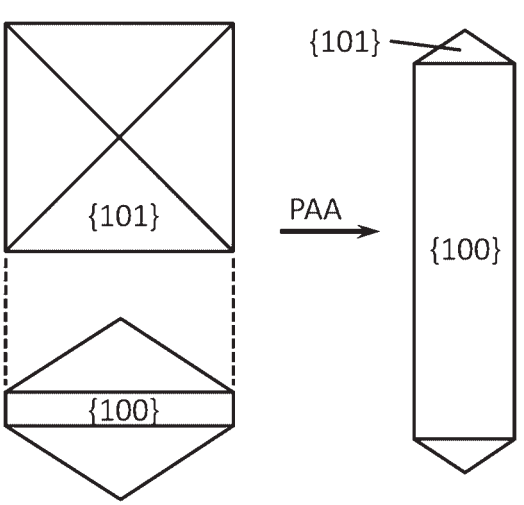

Figure 3 Elongation of COD by PAA. Figure modified from Zhang et al., Chem Mater., 2002, 14, 2450.[26]

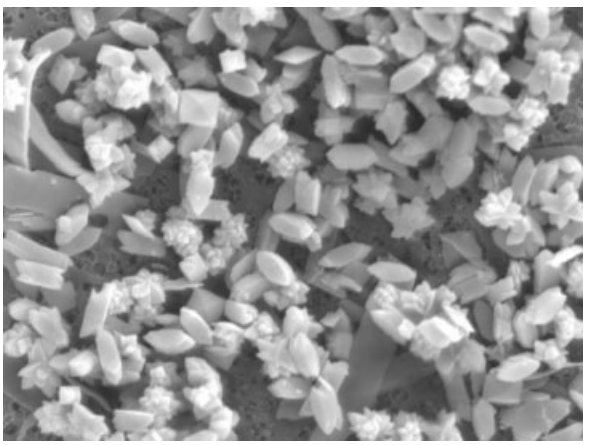

Figure 4 Crystal morphologies in the absence of PAA. COD and COM crystals formed in the absence of polymer after 120 min, 52.8 μm across image.

proceeding from solution or melt, rather than the polymorph of greatest thermodynamic stability. They are also consistent with previous experimental observations of calcium oxalate hydrates.[28,5]

Crystal morphologies in the presence of PAA

Table II presents a description of the phase, morphology, and crystal sizes of calcium oxalate crystals obtained in the presence of PAA at 23°C. Unlike the crystallization carried out in the absence of polymer, none of the crystallizations carried out in the presence of PAA gave rise a predominant COM phase. The crystals appearing in the micrographs could be characterized as a hierarchy of crystal populations, consisting of mainly COD and COT phases. In experiments carried out at 90°C, all crystals observed were well-formed COM for all PAA, consistent with a more rapid transition to the thermodynamically favourable product.

The crystal distributions have been divided into three populations, *viz.*, A, which is predominantly COT; B, consisting of COD crystals; and C, consisting of a mixture of ill-formed COT and small crystals of elongated COD.

Population A

The largest population observed in most preparations was of ribbon-like structures, 3–8 μm wide, often curved and variable in length from slightly longer than their width to 30–40 μm (Fig. 5). XRD results suggest that this phase was COT, and consistent with Ostwald's rule of stages this phase forms rapidly. In most cases, the size and morphology of these crystals did not change significantly over the course of the precipitation.

Population B

This population consists primarily of particles of D_{4h} symmetry that are clearly COD (Fig. 6). These typically grew over time and became more distinct, but in some cases gave rise to extensive surface nucleations leading to stellate structures. The crystals in this population were in almost all cases considerably smaller than the first population, typical dimensions being 3 μm × 3 μm.

Population C

This is the smallest population, which was not present in all crystallizations and was the most variable in composition and over time. At longer crystallization times especially, small crystals like lengths of ribbon were observed, which had ragged edges instead of the well-defined edges seen in the large ribbons of COT (Fig. 7). These were typically of dimensions 1 μm × 2 μm, and may provisionally be identified as a deformed COM morphology. 'Little spindles' were observed which may be the short ribbon-like crystals seen from the side.

Also primarily at long times, small crystals of COD were observed in many experiments. These crystals were frequently elongated (Fig. 8). These were frequently accompanied by small stellates, typically of order 1 micron square and attributed to heterogeneous nucleation.

Confirmation of the morphology assignments was done by powder XRD of the Series 1 preparations with the intermediate-length PAA inhibitors (Table III, Fig. 9). These results also show that the plate and ribbon-like morphologies dominating at long times for most preparations in the presence of PAA are primarily COT, rather than the COM which is the primary product in the absence of PAA.

The effect of different PAAs on the crystal morphology and the speciation may be summarized as follows:

- **COT is the main phase**. In the control experiment without polymer, COM is the main product. However, the HB samples contains COD as the predominant phase.
- **Different proportions of COD**. Most samples have much more of the initially-formed COT population A than of the population B of smaller crystals dominated by COD. However, the hexyl end-group (i.e., HB) gives rise to a population dominated by COD.
- **COD crystal development.** In some preparations these began rounded and became sharp over time, while in others they remained rounded at all times. The observation of COD formation is consistent with previously

TABLE II
Effect of PAA End-Groups on Calcium Oxalate Crystal Morphologies

Series 1

PAA	A-type population COT	B-type population COD	C-type population Mixture of COD and COM
EB 2000	Regular, 5–10 μm wide.	Initially rounded, becoming well defined at 120 min. Some stellates.	At 120 min, much elongated COD at 1× 2 aspect ratio and stellates.
EB 4000	3–4 μm wide at 2 min, 4–6 μm wide at 120 min.	Few present. Initially moderately well-formed, never well-defined.	Variable and poorly formed. No elongated COD visible.
EB 6000	Well-formed, 2–4 μm wide.	Few present. Rounded at all times.	Very few present.
HB 2000	Negligible at all times.	Initially poorly formed, well defined at 120 min. Numerous, with significant heterogeneous nucleation.	At 120 min, much elongated COD at 2 × 3 aspect ratio and stellates.
HB 4000	Short, well-formed, 8–9 μm wide, few in number.	Many, still indistinct even at end.	Small population of small COD.
HB 6000	Highly irregular in length and width. Much more numerous than in HB 2000 and HB 4000.	Initially poorly formed, distinct at end.	At 120 min, primarily COD, with elongated aspect ratio close to 1×1.
CB 2000	Mostly short, 5–6 μm wide. Some longer curved ones, numerous aggregates.	Few. Initially rounded. Well-defined late, variable in size.	Some elongated COD at 120 min, aspect ratio 3 × 2.
CB 4000	Variable with respect to width, mostly short.	Initially poorly formed, distinct at end. Some twinning.	Some stellates, much elongated COD after 50 min, variable in size of aspect ratio about 1 × 2.
CB 6000	Fairly narrow. Variable in length.	Very few. Initially poorly-formed, distinct at end.	A few short fat elongated CODs (aspect ratio 1×1 or less).
DB 2000	3–4 μm wide, variable length.	Moderately numerous, amorphous early, sharp at end	A few elongated COD, aspect ratio 3× 2.
DB 4000	Fairly regular, 5–7 μm wide.	Initially poorly-formed, distinct at end. Some elongated.	Many distinctive elongated COM, often clustered, aspect ratio 1 × 5.
DB 6000	Short and irregular. 3–4 μm wide at 2 min, 5–6 μm wide at 80 min.	Moderate numbers, become more distinct with time but still largely indistinct at 80 min.	Few visible.
HDB 2000	Irregular in width and length. 2–4 μm wide.	Very few COD, at 40 min and after.	Not observed.

Series 2

PAA	A-type population COT	B-type population COD	C-type population Mixture of COD and COM
EB 2000	Highly variable.	Initially rounded, become well-defined at 120 min. Some stellates.	Many ribbon and spindle structures at 2 min. Much reduced with some stellates at 120 min.
EB 4000	Narrow (2–4 μm), variable, often aggregated.	Rounded at all times. Numerous stellates, little change with time.	Ragged shapes and some stellates.
EB 6000	Highly variable.	Few present. Rounded at all times.	Many spindles/ribbons, very regular. about 0.6 × 1.2 μm.
HB 2000	Short, poorly formed, 6–7 μm wide.	Initially indistinct, moderately defined later, with some elongated.	At 120 min, mix of ribbon structures, spindles, stellates, and some elongated COD, aspect ratio 1 × 5. A few ribbon structures at 2 min.
HB 4000	Narrower (4–5 μm) and more numerous than S1 population.	Initially poorly-formed, distinct at end.	At 120 min, mixture of ribbons and stellates. Ribbon structures at 2 min.
HB 6000	Highly irregular in length and width. Much more numerous than in HB 2000.	Few. Initially rounded. Some large and well-defined late, others rounded.	Mostly ribbons. Some very small elongated COD at 120 min, about 1 × 2–3 aspect ratio.
CB 2000	Mostly short, 5–6 μm wide. Some longer curved ones, numerous aggregates.	Initially poorly-formed, distinct at end. Much twinning and stellates.	Many spindles and ribbon structures at all times.
CB 4000	Narrower and more regular than Series 1.	Few. Initially well-defined, some slightly elongated.	Elongated COD, aspect ratio about 1 × 3
DB 2000	Highly variable.	Numerous, mostly rounded at all times.	Numerous ribbons.
DB 4000	Irregular, variable width.	Few, rounded at all times.	Numerous ribbons and spindles.
DB 6000	As DB 6000 S1, more small irregular structures.	Moderate numbers, indistinct at all times, stellates.	Many ragged ribbon structures.

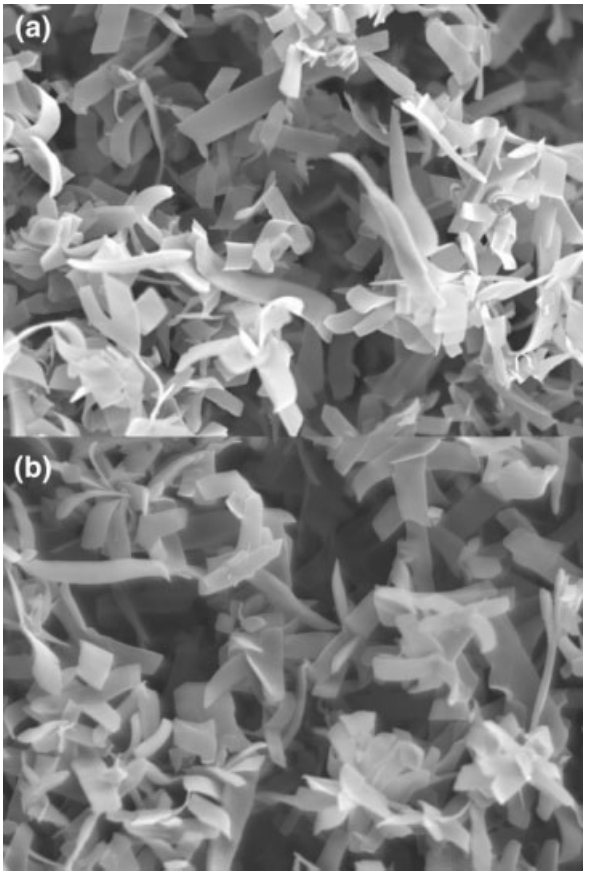

Figure 5 Calcium oxalate population A. (a) Series 1, EB1, 120 min, 88 μm across image, showing dominant ribbon-like COT morphology. (b) Series 1, DB3, 40 min, 88 μm across image, showing dominant ribbon-like COT morphology.

observed effects of synthetic and biological polycarboxylic acids.[19,24] COD crystals were typically poorly developed in the early stages of the experiment, with rounded vertices, but were observed to have sharper vertices in the later stages of the experiments.

- **Elongated COD habit in population C.** The degree of elongation of COD appeared to be fairly constant within each sample. The formation of elongated COD morphology was evident in experiments with the additives EB1, DB2, HB1, HB3, and the CB series.

In general, there was relatively little difference in morphology of crystal formed in Series 1 and Series 2, suggesting the morphologies and crystal sizes were not defined primarily by the nucleation process.

Series 1

In general, most Series 1 experiments gave COT as the main final product, rather than the COM

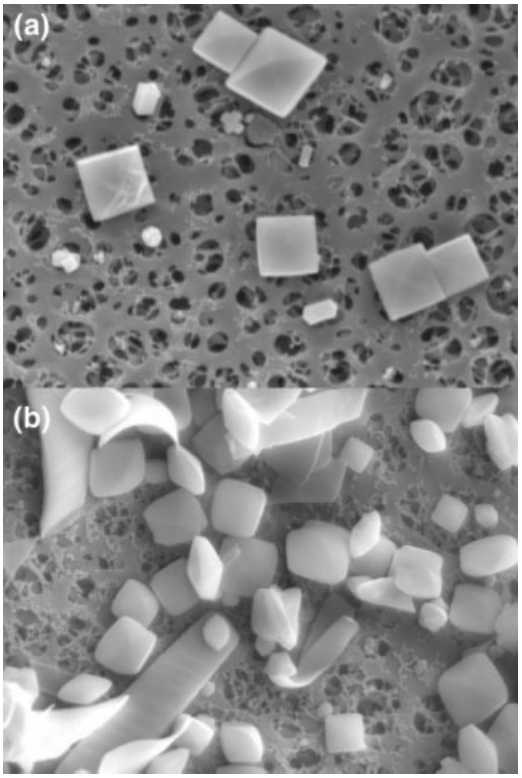

Figure 6 Calcium oxalate population B. (a) Series 1, EB1, 120 min, 33 μm across image, showing well-formed COD crystals. (b) Series 1, DB3, 40 min, 33 μm across image, showing rounded COD crystals.

observed in the control. XRD results are consistent with a small proportion of COM in crystals prepared with some of the additives, but none of the Series 1 samples were dominated by COM to the same extent as the control sample. A larger proportion of COD was also observed in many of the Series 1 experiments than the control experiments, an observation consistent with previously observed effects of synthetic and biological polycarboxylic acids.[19,24]

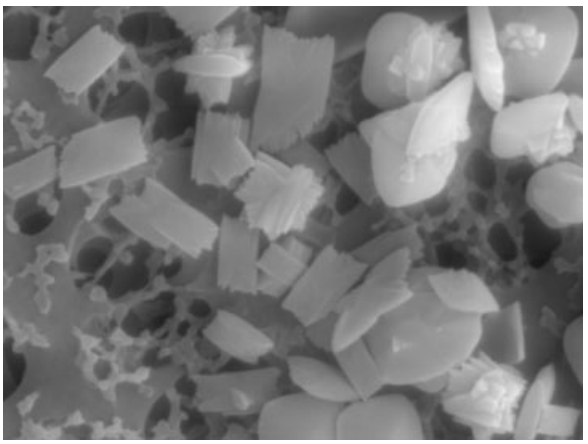

Figure 7 Calcium oxalate population C. Series 2, DB3. 2 min, 11 μm across image, showing ragged-ended forms of COM.

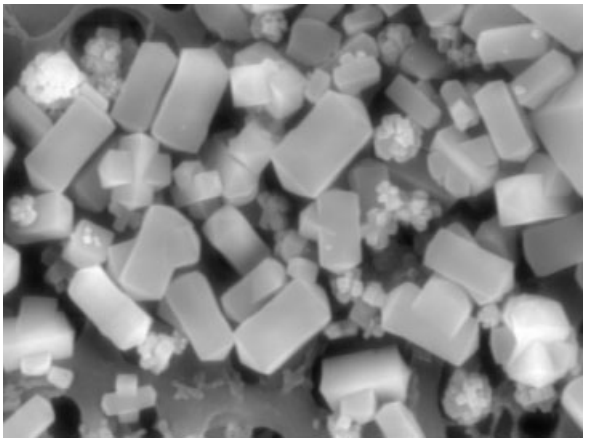

Figure 8 Calcium oxalate population C. Series 1, EB1, 120 min, 11 μm across image, showing elongated COD crystals and stellates.

COD crystals were typically poorly developed in the early stages of the experiment, with rounded vertices, but were observed to have sharper vertices in the later stages of the experiments. As the experiments were continued, the elongated COD crystal morphology also became evident in experiments with additives EB1, DB2, HB1, HB3, and the CB series.

In polymers HB1 and HB2, a clear majority of the crystals formed were COD rather than COT. These experiments were associated with an early onset of significant crystal growth as measured by conductivity, but a long crystallization time suggesting much slower crystal growth in these systems.[23]

There is considerable experimental evidence suggesting that optimal efficiency of inhibition by polyacrylic acid scale inhibitors is given by polymers of intermediate molecular mass, 2000–4000.[20,29] Our researches on the calcium oxalate system suggest that the position of this optimum shifts to longer molecular mass as the size of the end-group increases, and this correlates well with the polymers giving the greatest amount of elongated COD in Series 1.

Series 2

In general, there was relatively little difference in morphology of crystals formed in Series 2 from Series 1, suggesting the observed morphologies were not determined by nucleation. All tests in Series 2 formed COT as the major morphology. All tests also formed COD which had rounded vertices after 2 min of crystallization and sharp vertices after 120 min. Where the {100} face on the COD could be clearly delineated, it was larger in this series than in Series 1. Boat COM crystals also formed in all tests and were of the same approximate size (1.5 μm × 0.8 μm × 0.7 μm) as crystals found in the control after 30 s of crystallization.

In HB1, CB1, and CB2, the elongated COD morphology was observed after long times and in HB4 COD rather than COT was the predominant morphology at long times.

DISCUSSION

The primary calcium oxalate species obtained under most circumstances was COT, rather than the COM obtained in the absence of polymer. With the HB polymers, however, COD was the predominant phase, suggesting that end-groups play a crucial role in the action of PAA as crystallization modifiers.

If polymeric crystallization inhibitors are acting primarily by adsorption to growing crystal surfaces, then a molecular mass dependence on effectiveness is expected, as small chains will desorb rapidly and large chains will not relax sufficiently to cover the surface within the required timeframe and leave

TABLE III
Effect of PAA End-Groups on the Distribution of Calcium Oxalate Phases, Series 1

Experiment	Peak area, COT (d = 6.63 Å)	Peak area, COM (d = 5.90 Å)	Peak area, COD (d = 6.18 Å)	%COT	%COM	%COD
Control 120 min	0	4200	1015	0	81	19
EB2 2 min	5233	0	0	100	0	0
EB2 120 min	13,080	0	0	100	0	0
HB2 2 min	0	0	1144	0	0	100
HB2 40 min	1523	0	2467	38	0	62
HB2 80 min	1284	0	1615	38	0	62
HB2 120 min	1126	0	1159	49	0	51
CB2 2 min	3134	0	0	100	0	0
CB2 120 min	4452	0	2788	62	0	38
DB2 2 min	2461	0	0	100	0	0
DB2 2 min	36,392	1153	0	97	3	0
DB2 120 min	5120	2544	0	100	0	0
HDB2 2 min	23,753	1021	0	96	4	0
HDB2 120 min	28851	1391	0	95	5	0

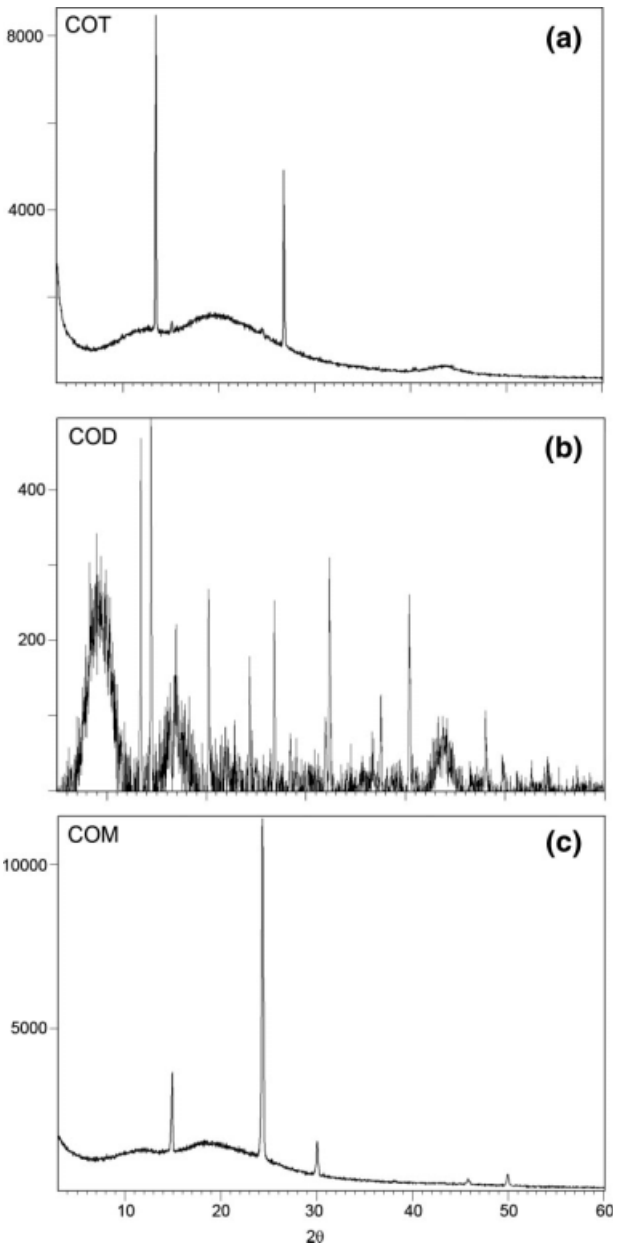

Figure 9 XRD Diffractograms of precipitated calcium oxalate. (a) Series 1, HDB2, 2 min, primarily COT, (b) Series 1, HB2, 40 min, primarily COD, (c) 90°C, CB1, 120 min, primarily COM.

dangling loops and coils on the crystal surface.[20,22] This optimum mass of the polymer typically lies between 2000 and 4000 g/mol.[21] Inclusion of an end-group that does not contain functionalities, which can interact significantly with the crystal might be expected to encourage desorption, shifting the point of maximum effectiveness to greater polymer molecular mass. Hence, if surface adsorption was the primary mechanism of action of the inhibitors, the effect of HB terminated PAA might naively be expected to be intermediate between the effects of EB and DB terminated PAA. Instead, dramatic variations in behavior were observed, with HB1 and HB2 tests leading to formation of the less stable COD over the more stable COM (The free energy of formation of COM and $H_2O_{(l)}$ = –1751 kJ/mol[30] and of COD = –1744 kJ/mol[31]), while both EB and DB terminated polymers led to stabilization of the kinetically favored COT and its retention as the majority species after times at which it is entirely replaced by COM in the absence of PAA. In general, the COD crystals formed in the presence of HB and CB terminated PAA were more sharply defined than COD crystals formed in the presence of other PAA.

Further consideration of the probable effect of a hydrophobic end-group on polymer absorption suggests that as the size of the end-group increases, as well as impacting negatively on adsorption to a charged surface it will be more and more unfavorable for it to exist in the aqueous phase, and it would be expected to remain in an environment where there is a high concentration of polymer and it may self-associate with other hydrophobes. This suggests that the HB and CB end-groups associated with more defined COD morphology, a shorter aspect ratio in the elongated COD and a greater proportion of COD are those which most encourage desorption of the polymer from calcium oxalate micro-crystallites.

Zhang et al.[26] attributed the elongated COD morphology to the adsorption of polymer to the {100} faces of the COD crystal, causing the face to grow slowly and increase in size. Thus weaker adsorption would be expected to lead to a less elongated COD morphology.

The differences in speciation must be related to preferential adsorption of PAA to one polymorph. However, it is not immediately clear which polymorph is preferred from the observations. Inhibition of COM relative to COT and COD formation may be related either to stabilization of the initially formed COT species, or inhibition of the growth of COM. Initial polymer adsorption onto COT surfaces may retard their conversion to more thermodynamically stable forms of calcium oxalate by stabilizing the ion spacing at the surface; thus, it would be natural for more COD to be observed with those polymers which bind more weakly to calcium oxalate in general, allowing more growth of COD nuclei. It has been reported that urinary tract proteins—material perhaps not very analogous to PAA, but also likely to be anionic polyelectrolytes *in vivo*—show weaker adhesion to COD than COM.[32]

Structurally, COM and COT are more similar to each other than they are to COD,[33] and if PAA is binding to COT it would be expected to bind preferentially to COM surfaces as they form and retarding their growth relative to COD. This is consistent with the investigations of Jung et al. which demonstrated that PAA is very effective in retarding growth on

the {121} and {021} faces of COM and slows growth on the {100} faces more effectively than the {010} faces, a combination which would be expected to lead to a broken-ribbon-like morphology as seen in crystal population C. Mechanistically this is related to the distribution and spacing of the ions on the different surfaces: {010} faces present chiefly oxalate ions, while a dense pattern of calcium ions is presented at {100} faces.[34] Adsorption of PAA to COM nuclei appears to be rapid and irreversible, from the failure of the boat COM to grow significantly in the presence of polymer. Differential degrees of absorption to COD interfaces could then explain the greater reduction in crystal growth rate seen with HB-terminated PAA and the preferential generation of COD in these systems.

Huang et al. have carried out experiments with calcium carbonate and poly(acrylic acid) analogous to these at 30°C and pH = 8.5 using significantly larger amounts of PAA, with one series where the PAA was initially present and another where it was added after nucleation, and only observed inhibition of crystallization and changes in preferred polymorph in the former case.[35] This suggests the PAA is consumed in the nucleation process in the formation of calcium carbonate under these conditions, in contrast to the results reported here. This may be connected with the higher $[Ca^{2+}]$: [anion] ratio employed in this work, which would tend to favor desorption, or it may reflect an intrinsic difference between the calcium carbonate and calcium oxalate surfaces.

CONCLUSION

Significant differences in calcium oxalate speciation and crystal morphology were observed in systems that varied only in the molecular mass and end-group functionality of the PAA scale inhibitor used. The dependence of the changes in the crystals formed on the end-group functionality was more pronounced than the molecular mass dependence, with mid-sized hydrophobic end-groups giving a larger proportion of COD, more clearly-formed COD crystals, and a population of small elongated COD crystals which was less elongated than analogous crystals formed with both more hydrophobic and less hydrophobic end-groups. These features can be explained by postulating that the adsorption and desorption of the PAA from calcium oxalate surfaces in this system is dominated by the nature of the end-group, rather than its molecular mass. A plausible molecular mechanism for this would be the association of hydrophobes to form dynamic supermolecular structures retarding desorption, not primarily in the bulk phase where PAA concentration is low, but at the crystal surfaces where the concentration of polymer is high.

The authors gratefully acknowledge the assistance of Patrick Littlefield of the University of New England in the collection of the SEM images.

References

1. Yu, L.; Ni, Y. Tappi J 2006, 5, 9.
2. Weaver, M. L.; Qiu, S. R.; Hoyer, J. R.; Casey, W. H.; Nancollas, G. H.; De Yorec, J. J. Chem Phys Chem 2006, 7, 2081.
3. Grohe, B.; O'Young, J.; Ionescu, D. A.; Lajoie, G.; Rogers, K. A.; Karttunen, M.; Goldberg, H. A.; Hunter, G. K. J Am Chem Soc 2007, 129, 14946.
4. Akyol, E.; Oener, M. J Cryst Growth 2007, 307, 137.
5. Yu, H.; Sheikholeslami, R.; Doherty, W. O. S. Powder Technol 2005, 160, 2.
6. Yu, H.; Sheikholeslami, R.; Doherty, W. O. S. AIChE J 2005, 51, 1214.
7. Yu, H.; Sheikholeslami, R.; Doherty, W. O. S. AIChE J 2005, 51, 641.
8. Yu, H.; Sheikholeslami, R.; Doherty, W. O. S. Chem Eng Sci 2002, 57, 1969.
9. Doherty, W. O. S.; Crees, O. L.; Senogles, E. Cryst Res Technol 1995, 30, 791.
10. Doherty, W. O. S.; Crees, O. L.; Senogles, E. Cryst Res Technol 1993, 28, 603.
11. Doherty, W. O. S. Ind Eng Chem Res 2006, 45, 642.
12. Donnet, M.; Jongen, N.; Lemaitre, J.; Bowen, P. J Mater Sci Lett 2000, 19, 749.
13. Olmstead, M. M.; Bria, L. E. Chemtracts 2006, 19, 193.
14. Donnet, M.; Jongen, N.; Lemaitre, J.; Bowen, P.; Hofmann, H. Int Symp Ind Cryst 1999, 14, 717.
15. Streit, J.; Tran-Ho, L.-C.; Koenigsberger, E. Monatsh Chem 1998, 129, 1225.
16. Yu, J.; Tang, H.; Cheng, B. J Colloid Interface Sci 2005, 288, 407.
17. Akyol, E.; Bozkurt, A.; Oner, M. Polym Adv Technol 2006, 17, 58.
18. Benítez, I. O.; Talham, D. R. J Am Chem Soc 2005, 127, 2814.
19. Jung, T.; Kim, W.-S.; Kyun Choi, C. J Cryst Growth 2005, 279, 154.
20. Geffroy, C.; Persello, J.; Foissy, A.; Lixon, P.; Tournilhac, F.; Cabane, B. Colloids Surf A 2000, 162, 107.
21. Binglin, Y. Water Treat 1989, 4, 257.
22. Doherty, W. O. S.; Fellows, C. M.; Gorjian, S.; Senogles, E.; Cheung, W. H. J Appl Polym Sci 2004, 91, 2035.
23. Wallace, A. G.; Fellows, C.; Doherty, M. J App Polym Sci, submitted.
24. Jung, T.; Sheng, X.; Choi, C. K.; Kim, W.-S.; Wesson, J. A.; Ward, M. D. Langmuir 2004, 20, 8587.
25. Qiu, S. R.; Wierzbicki, A.; Orme, C. A.; Cody, A. M.; Hoyer, J. R.; Nancollas, G. H. Proc Natl Acad Sci 2004, 101, 1181.
26. Zhang, D.; Qi, L.; Ma, J.; Cheng, H. Chem Mater 2002, 14, 2450.
27. Threlfall, T. Org Process Res Dev 2003, 7, 1017.
28. Brečević, L.; Škrtić, D.; Garside, S. J Cryst Growth 1986, 74, 399.
29. Senogles, E.; Doherty, W. O. S.; Crees, O. L. In Encyclopedia of Polymer Science and Technology; Kroschwitz, J., Ed. Wiley-Interscience: Boca Raton, 1996; pp 7587–7594.
30. Aylward, G.; Findlay, T. SI Chem Data 2001,
31. Weast, R. E., Ed. Handbook of Chemistry and Physics; Chemical Rubber Publishing Company: Boca Raton, 1967.
32. Sheng, X.; Ward, M. D.; Wesson, J. A. J Am Soc Nephrol 2005, 16, 1904.
33. Echigo, T.; Kimata, M.; Kyono, A.; Shimizu, M.; Hatta, T. Miner Mag 2005, 69, 77.
34. Tunik, L.; Addadi, L.; Garti, N.; Furedi-Milhofer, H. J Cryst Growth 1996, 167, 748.
35. Huang, S.-C.; Naka, K.; Chujo, Y. Polym J (Tokyo) 2008, 40, 154.